Journal of Fluorine Chemistry 135 (2012) 75–82

Contents lists available at SciVerse ScienceDirect

Journal of Fluorine Chemistry

journal homepage: www.elsevier.com/locate/fluor

Fluorine-containing thermo-sensitive core/shell microgel particles: Preparation, characterization, and their applications in controlled drug release

Guoqiang Liu [a], Xiaolong Li [a], Shengdong Xiong [a], Ling Li [a], Paul K. Chu [b], Shuilin Wu [a,b], Zushun Xu [a,b,*]

[a] Ministry-of-Education Key Laboratory for the Green Preparation and Application of Functional Materials, Hubei University, Wuhan 430062, China
[b] Department of Physics & Materials Science, City University of Hong Kong, Tat Chee Avenue, Kowloon, Hong Kong, China

ARTICLE INFO

Article history:
Received 5 July 2011
Received in revised form 20 August 2011
Accepted 24 August 2011
Available online 1 September 2011

Keywords:
Thermo-sensitive
Fluoropolymer
Microgels
Core/shell
Controlled drug release

ABSTRACT

A novel series of fluorine-containing thermo-sensitive core/shell microgel particels, poly[N-isopropylacrylamide-co-2,2,3,4,4,4-Hexafluorobutyl methacrylate-co-Poly(ethylene glycol) methyl ether methacrylate] [P(NIPAAm-co-HFMA-co-MPEGMA)], were prepared via surfactant free emulsion polymerization. The composition of the copolymer microgels was characterized by FTIR, ^{1}H NMR, and ^{19}F NMR. Subsequently, the thermo-responsive behavior of the microgels was studied by UV–vis spectroscopy, fluorescence spectroscopy, dynamic light scattering, and transmission electron microscopy. The copolymer microgels exhibited a lower critical solution temperature (LCST) above the normal human physiological temperature. When the temperature was above the LCST, the hydrophobicity of the microgels increased significantly, and the average hydrodynamic diameter decreased greatly. TEM results showed that the copolymer microgels formed loose core–shell spherical particles below the LCST, but above the LCST, the particles became compact and the core–shell structure was not obvious. The drug loading and *in vitro* release were studied with 5-fluorouracil as a model drug. The result showed that the rate and amount of the drug release became much higher above the LCST. In a word, the study indicated that the fluorine-containing thermo-sensitive copolymer microgels had promising potential applications as a "smart" drug carrier in biomedical field.

1. Introduction

Responsive microgels will undergo phase transition behavior in response to changes in environmental conditions such as temperature, pH, electric field, and magnetic field [1–5]. Due to many varied potential application, the thermo-sensitive microgels have received significant attention in the past scientific literature [6–8]. Thermo-sensitive microgels have a specific lower critical solution temperature (LCST), at which the microgels will show a volume phase transition. When the temperature is below the LCST, the microgels exist in the swelling state, and above the LCST, the shrinkage will occur. Compared with macroscopic gels, thermo-sensitive microgels show a more rapid swelling/collapse behavior as a result of a larger surface area. These properties make thermo-sensitive microgels have potential applications in the fields of drug delivery vehicles, biological probe, biosensor and other biotechnology [9–11]. As the microgels have been extensively studied, the core–shell thermo-sensitive microgel particles have attracted much attention for their pharmaceutical applications in recent years [12,13].

Poly(ethylene glycol) (PEG) is a low cost commercial product that possesses some unique and outstanding properties such as hydrophilicity, biocompatibility, nontoxicity, lack of immunogenicity, metal complexing ability, as well as solubility in water and organic solvents [14–17]. If PEG serves as the shell chains of microgel particles, not only will the biocompatibility of microgels be improved, but also their response to temperature will become more sensitive due to the good spatial degrees of freedom of polymeric chains [18–20].

Fluoropolymers have many unique characteristics such as high hydrophobicity, high thermal and mechanical stability, gas dissolving capacity, high fluidity, low dielectric constants, oil- and water-repellency, and very interesting surface properties [21–27]. If the core chains of microgel particles contain fluorinated segment, not only will the microgels exhibit some special response characteristics, but also the binding force between microgels and hydrophobic drugs will increase [28].

Poly(N-isopropylacrylamide) (PNIPAAm) is a typical thermo-responsive polymer and shows a lower critical solution temperature of approximately 32 °C in aqueous solution [29]. The thermo-sensitive copolymers based on PNIPAAm have been extensively reported [30–33], but the core/shell thermo-sensitive microgel

* Corresponding author at: Ministry-of-Education Key Laboratory for the Green Preparation and Application of Functional Materials, Hubei University, Wuhan 430062, China. Tel.: +86 27 61120608; fax: +86 27 88665610.
E-mail address: zushun25@hubu.edu.cn (Z. Xu).

0022-1139/$ – see front matter © 2011 Elsevier B.V. All rights reserved.
doi:10.1016/j.jfluchem.2011.08.012

particles, whose shells are composed of PEG and whose cores contains fluorinated segments, have not been studied.

In this study, the fluorine-containing thermo-sensitive core/shell microgels P(NIPAAm-*co*-HFMA-*co*-MPEGMA) were prepared via surfactant free emulsion polymerization to obtain controlled and narrow size core–shell structures. The thermo-responsive behavior of the copolymer microgels was studied by UV–vis spectrophotometer, spectrofluorimeter, dynamic light scattering instrument, and transmission electron microscopy. The results showed that the change of temperature had a significant impact on the morphology and size of microgel particles. Furthermore, the cytotoxicy were evaluated via MTT viability assay, indicating that the copolymer microgels had low toxicity. Besides, the drug loading and *in vitro* drug release of 5-fluorouracil (5-FU) with the microgels were studied in detail. The results showed that 5-FU was successfully incorporated into polymeric particles, and the change of temperature had a significant impact on the 5-FU release of drug-loaded microgels. Our study suggests that P(NIPAAm-*co*-HFMA-*co*-MPEGMA) microgel particles have a potential application as an "intelligent" drug carrier for controlled drug release.

2. Results and discussion

2.1. The composition of P(NIPAAm-co-HFMA-co-MPEGMA) copolymer microgels

Fig. 1 shows the FTIR spectrum of the copolymer microgels. The strong and wide absorption band at 3600–3200 cm^{-1} is attributed to the stretching vibration absorption of –NH– group. The absorption band at 2971.3–2873.8 cm^{-1} is assigned to the stretching vibration absorption of C–H in methyl and methylene. The characteristic absorption of ester carbonyl is observed at 1743.9 cm^{-1}, while the characteristic absorption of the carbonyl in amide group is observed at 1650.9 cm^{-1}. The peak at 1542.3 cm^{-1} is attributed to the stretching vibration absorption of C–N group. The peak at 1457.7 cm^{-1} is attributed to the bending vibration absorption. The double peaks at 1386.9 cm^{-1} and 1369.1 cm^{-1} are attributed to the absorption of two methyl in $–CH(CH_3)_2$ as a result of coupling vibration split. The characteristic absorption of C–F group is observed at 1188.2 cm^{-1}. The strong peak at 1104.5 cm^{-1} is assigned to the characteristic absorption of C–O in ether linkage. The emergence of these bands shows that temperature-sensitive monomer NIPAAm, fluorine-containing monomer HFMA and macromonomer MPEGMA all participate in the copolymerization. Besides, the characteristic absorption of C=C near 1630 cm^{-1} does not appear, indicating that the prepared product does not contain the unreacted monomers.

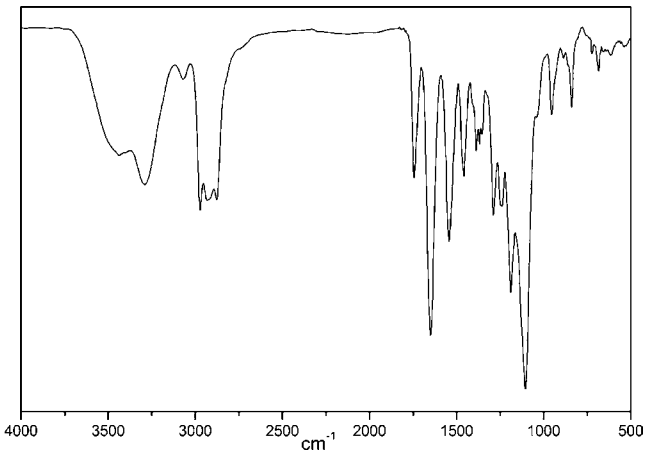

Fig. 1. FTIR spectrum of the copolymer P(NIPAAm-*co*-HFMA-*co*-MPEGMA).

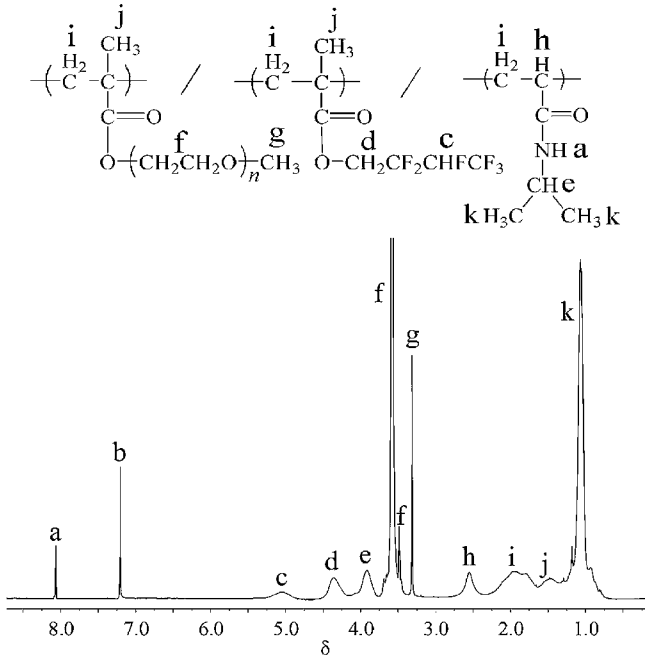

Fig. 2. ^{1}H-NMR spectrum of the copolymer P(NIPAAm-*co*-HFMA-*co*-MPEGMA).

Fig. 2 shows the ^{1}H NMR spectrum of the copolymer microgels. The peak at 7.21 ppm (b) is assigned to the solvent $CDCl_3$. The characteristic ^{1}H NMR signals of NIPAAm segment appear as follows: –NH– (a, δ = 8.06 ppm), –CH– (e, δ = 3.91 ppm) in $–CH(CH_3)_2$, CH_3– (k, δ = 1.06 ppm) in $–CH(CH_3)_2$. The characteristic ^{1}H NMR signals of HFMA segment appear as follows: $–CHFCF_3$– (c, δ = 5.04 ppm), $–OCH_2–CF_2$– (d, δ = 4.36 ppm). The characteristic ^{1}H NMR signals of MPEGMA as follows: $–CH_2CH_2O$– (f, δ = 3.58 ppm), CH_3O– (g, δ = 3.31 ppm). Besides, the signals of the copolymer main chain appear as follows: –CH– (h, δ = 2.55 ppm), $–CH_2$– (i, δ = 1.93 ppm), CH_3– (j, δ = 1.18–1.82 ppm). The copolymer compositions are calculated from the characteristic proton integrals. The NIPAAm, HFMA, and MPEGMA contents in the copolymers are calculated by the ^{1}H NMR peak intensity ratios of the –NH– protons of NIPAAm, the $–CH_2$– protons of HFMA, and the CH_3O– protons of the MPEGMA. Table 1 lists the copolymer compositions resulted from ^{1}H NMR.

To better characterize the structure of the copolymer, the ^{19}F NMR spectrum in Fig. 3 is used to determine the fluorocarbon moiety in the copolymer. There are three different kinds of fluorine resonances originating from the HFMA side chains in the copolymer. The signal at −75.3 ppm is assigned to the end $–CF_3$ group and the signal at −213.0 ppm is assigned to the $–CHF_2$ group. Because of the influence of the $–OCH_2$– group, the peak of $–OCH_2–CF_2$– splits into two peaks at −114.4 ppm and −120.3 ppm. The FTIR, ^{1}H NMR and ^{19}F NMR results confirm that the copolymer microgels have been successfully prepared.

Table 1
The compositions resulted from ^{1}H NMR for P(NIPAAm-*co*-HFMA-*co*-MPEGMA).

Sample	^{1}H NMR results (wt%)		
	PNIPAAm	PHFMA	PEG
N25F42-PEG33	24.7	42.9	32.4
N33F34-PEG33	34.1	34.7	31.2
N42F25-PEG33	41.5	25.8	32.7
N29F29-PEG42	30.2	29.3	40.5
N25F25-PEG50	24.3	26.4	49.3

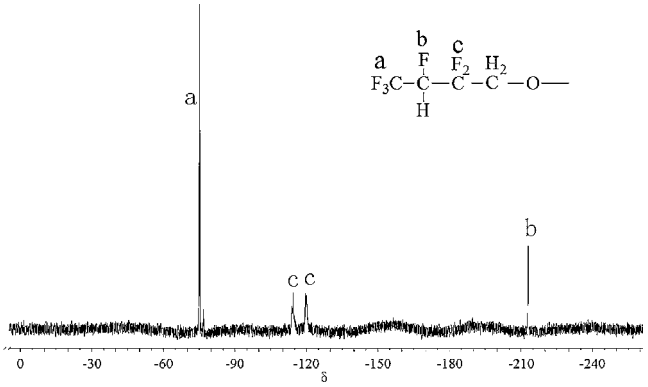

Fig. 3. ^{19}F-NMR spectrum of the copolymer P(NIPAAm-*co*-HFMA-*co*-MPEGMA).

2.2. LCST measurement

Poly(N-isopropylacrylamide) has a unique thermo-sensitive property in aqueous solution with its lower critical solution temperature (LCST) about 32 °C. Above the LCST, PNIPAAm changes from hydrophilicity to hydrophobicity, and shows a volume transition [29]. Due to the special characteristic, the copolymers based on PNIPAAm also have the temperature-responsive behavior.

As shown in Fig. 4, the initial transmittance of the copolymer microgels is not 100%, indicating that the microgel particles have existed at low temperature. As the temperature increases, the transmittance of copolymer emulsion decreases gradually. Specially, at low temperature the transmittance decreases slowly, but in a particular temperature range the transmittance decreases sharply. The LCST of the microgels are determined at the temperatures showing 50% of the initial transmittance.

As the temperature increases, the hydrogen bond between ether groups and water molecules is weakened, and the hydrophobicity of PEG side chains increases slowly [34,35]. Thus, the intramolecular and intermolecular hydrophobic association of copolymers becomes strong, leading to slight shrinkage of the microgel particles. The factor causes the transmittance of the copolymer emulsion to decrease slowly at low temperature. When the temperature comes to a special value (LCST), the PNIPAAm segments of the microgels exhibit a phase transition and the colloidal particles shrink significantly. Therefore, the transmittance falls sharply.

The LCST values of the prepared five samples are marked in Fig. 4. It is clear that with increasing the content of HFMA in the copolymer, the LCST decreases significantly, but the increase of PEG side chains leads to an increase in the LCST. As reported in the literature, the hydrophilic segments of copolymer lead to an increase in the LCST, while the hydrophobic segments lead to a decrease in the LCST [36,37]. In this work, the hydrophilic PEG chains can enhance the LCST of the copolymer microgels, and the hydrophobic HFMA segments can reduce the LCST. Thus, the LCST value of P(NIPAAm-*co*-HFMA-*co*-MPEGMA) can be changed by adjusting the monomer composition.

2.3. Fluorescence spectroscopy

The effect of temperature on the hydrophobicity of microgels is studied by the fluorescent probe technique. Nile red was a kind of hydrophobic fluorescent dyes and chosen as the probe molecular, because its fluorescence emission spectrum displays a strong environmental dependence [38]. The fluorescent intensity of Nile Red is negligible in an aqueous solution, while its fluorescence intensity increases significantly in the hydrophobic micro-environment. Fig. 5 shows the fluorescence spectra of Nile Red in the N33F34-PEG33 emulsion at different temperatures.

As shown in Fig. 5, with increasing the temperature, the fluorescence intensity increases gradually, but the wavelength of emission peak does not vary. Besides, when the temperature is below the LCST, the fluorescence intensity increase slightly, but when the temperature is above the LCST, marked changes in the intensity are observed. Below the LCST, there is a hydrophobic interaction between the fluorinated segments in the core of the microgels and Nile red, which leads to the increase in fluorescence intensity of Nile Red. Above the LCST, the NIPAAm segments show a phase transition from hydrophilicity to hydrophobicity, which enhance the hydrophobic interaction between the microgels and Nile Red significantly, so the fluorescence intensity increases obviously.

2.4. Dynamic light scattering

Thermo-sensitive microgel particles can shrink and swell in response to the changes in environmental conditions. To investigate the effect of temperature on the particles of P(NIPAAm-*co*-HFMA-*co*-MPEGMA) microgels, dynamic light scattering (DLS) technique is used to measure the average hydrodynamic diameter

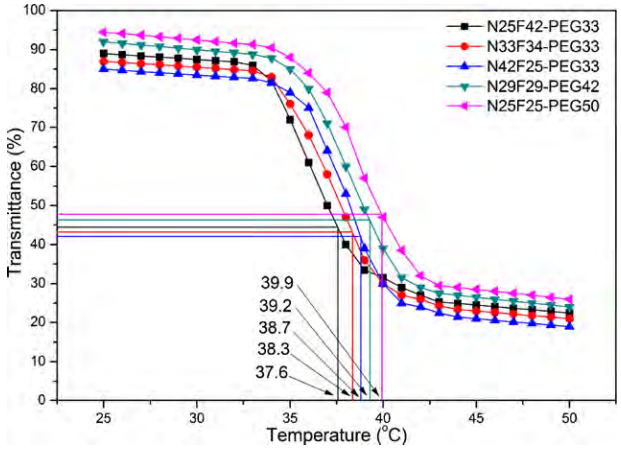

Fig. 4. Transmittance versus temperature plots for P(NIPAAm-*co*-HFMA-*co*-MPEGMA) with different monomer feed ratios. All the concentrations were kept at 1.0 mg/mL. The LCST values were marked in the figure.

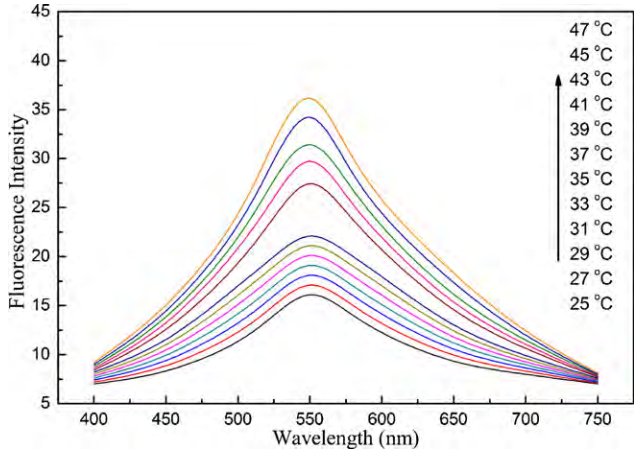

Fig. 5. Fluorescence spectra of Nile Red in the N33F34-PEG33 emulsion at different temperatures. The temperatures from bottom to top are 25 °C, 27 °C, 29 °C, 31 °C, 33 °C, 35 °C, 37 °C, 39 °C, 41 °C, 43 °C, 45 °C, and 47 °C. The concentarion of N33F34-PEG33 was kept at 1.0 mg/mL.

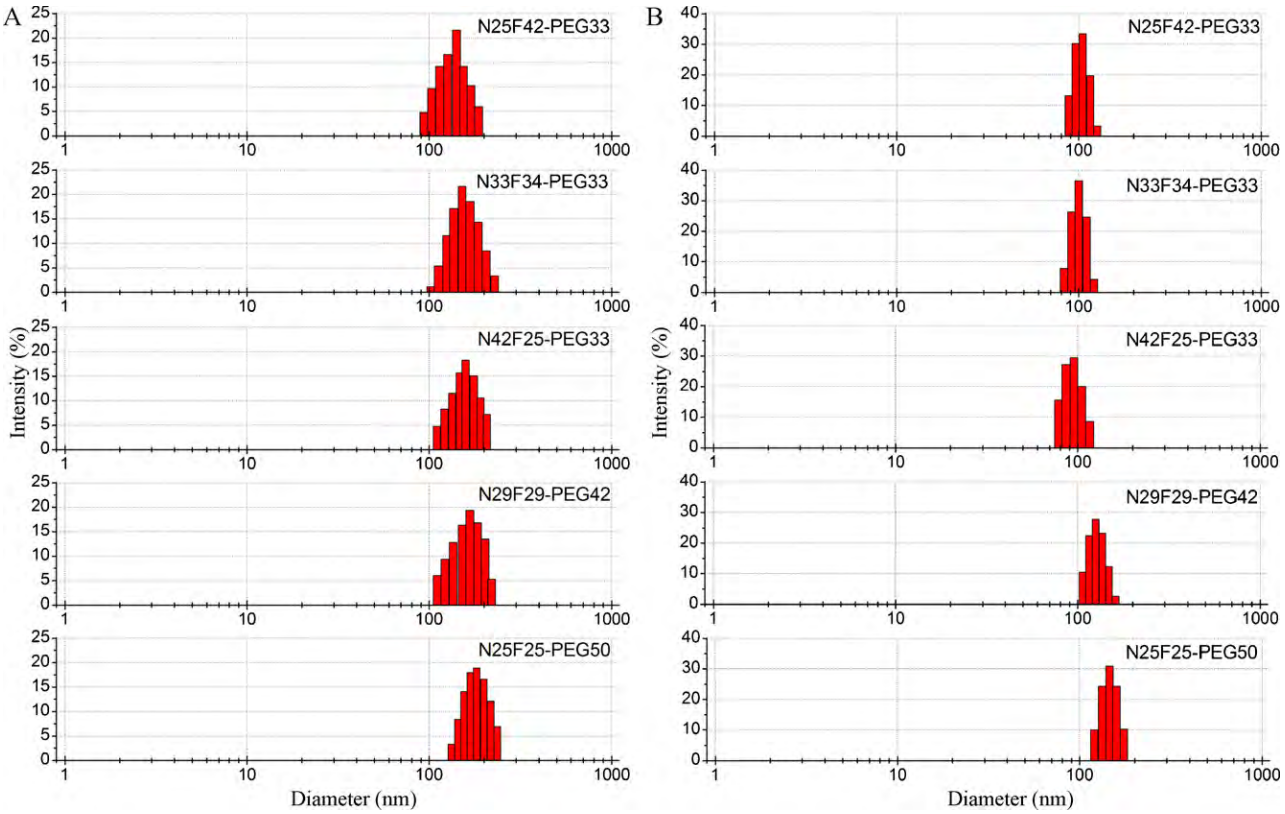

Fig. 6. Hydrodynamic diameters and distribution of P(NIPAAm-*co*-HFMA-*co*-MPEGMA) with different monomer feed ratios. The concentrations were all kept at 1.0 mg/mL, the measurement temperatures of (A) and (B) are 25 °C and 45 °C, respectively.

and size distribution at different temperatures. Fig. 6 shows the average hydrodynamic diameter and size distribution of P(NIPAAm-*co*-HFMA-*co*-MPEGMA) microgels at 25 °C and 45 °C, respectively. More specific values are listed in Table 2.

As shown in Fig. 6(A), at 25 °C (below the LCST), the diameter of the copolymer microgels is in the range of 140–180 nm, and their size distribution is relatively homogeneous. It is interesting that both the decrease of HFMA content and the increase of PEG chains lead to an increase in the microgel diameter. It can be explained by that the hydrophilic PEG side chains exist in the extension state in aqueous solution, while the hydrophobic fluorinated segments exist in the contraction state.

As shown in Fig. 6(B), at 45 °C (above the LCST), the diameter of the copolymer microgels is in the range of 90–140 nm. Compared with Fig. 6(A), the particle size of the five samples all decreases significantly. Above the LCST, NIPAAm segments of P(NIPAAm-*co*-HFMA-*co*-MPEGMA) microgels show a phase transition from hydrophilicity to hydrophobicity, which enhance the hydrophobic interaction. Thus, the obvious shrinkage of microgel particles occurs. Specially, as shown in Table 3, with increasing the content of NIPAAm segments or PEG side chains in the copolymer, the shrinkage degree increases gradually. This result shows that the shrinkage of the microgel particles is attributed to the temperature responsive groups.

Table 2
Hydrodynamic diameter, polydistribution index (PDI), and contraction amplitude for the P(NIPAAm-*co*-HFMA-*co*-MPEGMA) microgel particels.

Sample	Diameter (nm)		Contraction amplitude (nm)	PDI	
	25 °C	45 °C		25 °C	45 °C
N25F42-PEG33	140.2	104.7	35.5	0.249	0.178
N33F34-PEG33	151.4	101.9	49.5	0.235	0.181
N42F25-PEG33	159.5	93.3	66.2	0.282	0.165
N29F29-PEG42	168.1	129.5	38.6	0.231	0.172
N25F25-PEG50	180.3	143.6	36.7	0.264	0.169

Table 3
Monomer feed ratios, reaction temperature, reaction time, conversion and solid content for the copolymer P(NIPAAm-*co*-HFMA-*co*-MPEGMA).

Sample	NIPAAm (g)	HFMA (g)	MPEGMA (g)	Temperature (°C)	Time (h)	Conversion (%)	Solid content (%)
N25F42-PEG33	0.251	0.424	0.329	73	24	95.8	3.69
N33F34-PEG33	0.329	0.341	0.332	73	24	96.3	3.71
N42F25-PEG33	0.423	0.252	0.331	73	24	95.2	3.67
N29F29-PEG42	0.292	0.289	0.333	73	24	96.4	3.71
N25F25-PEG50	0.253	0.251	0.331	73	24	96.1	3.70

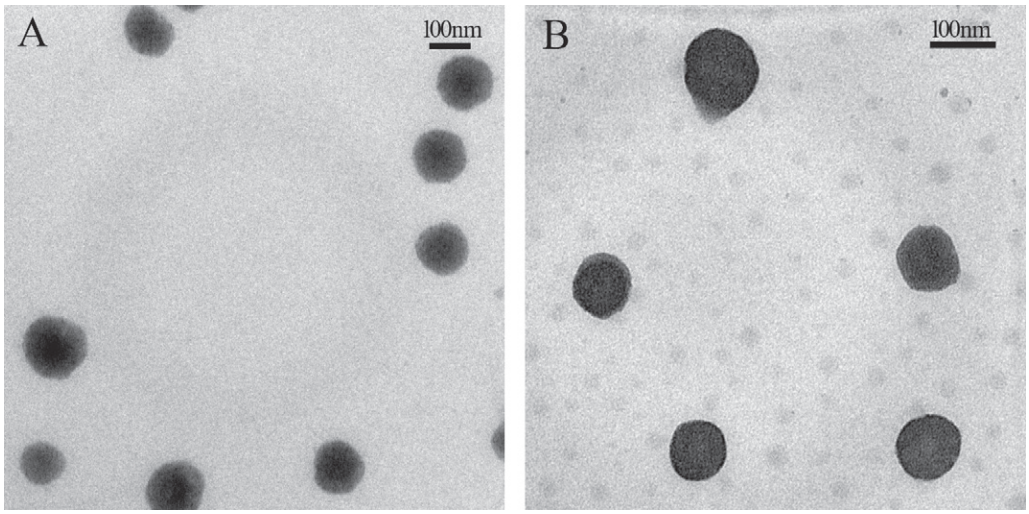

Fig. 7. TEM morphology of N33F34-PEG33 microgel particles with the concentration of 1.0 mg/mL. (A) The sample was dried under vacuum at 25 °C; (B) The sample was dried under vacuum at 45 °C.

2.5. Transmission electron microscopy

To observe the morphology of microgel particles intuitively and study the effect of temperature on the morphology, the N33F34-PEG33 microgels are investigated by transmission electron microscopy at 25 °C and 45 °C, respectively. Fig. 7 exhibits the TEM images of the copolymer microgels at different temperatures.

As shown in Fig. 7(A), at 25 °C the N33F34-PEG33 microgels form spherical particles with a core–shell structure, whose size is about 150 nm. Below the LCST, due to the hydrophobic characteristic of the fluorinated segments and the cross-linked structure between PHFMA and PNIPAAm, during the formation process of particles, PHFMA and PNIPAAm segments have a high tendency to bury themselves in the interior of the microgel particles as the core [39]. Meanwhile the PEG side chains serve as an outer hydrophilic shell stabilizing the particles.

As shown in Fig. 7(B), at 45 °C the morphology and particle size of microgels undergo significant changes. The core–shell structure is not obvious, and the particle size become smaller compared with that in Fig. 7(A). On the one hand, above the LCST, the PNIAAm shows a phase transition, leading to the shrinkage of microgel cores. On the other hand, with the increase of temperature, the PEG chains become hydrophobic gradually, leading to the collapse of microgel shells. Therefore, the core–shell structure disappears, and the particle size becomes smaller.

Based on the analysis above, the P(NIPAAm-*co*-HFMA-*co*-MPEGMA) microgel particles with a amphiphilic core–shell structure display a desired thermo-responsive behavior, which provides a possibility for the microgels as thermo-sensitive drug carrier. The cross-linked core may serve as a tiny drug warehouse, which encapsulates the hydrophobic drug by chemical bonding or physical embedding. Meanwhile, the hydrophilic shell not only stabilizes the drug carrier but also improves the biocompatibility of drug-loaded particles. Below the LCST, because of the hydrophobic interaction, the hydrophobic drugs may be stored in the cores of microgels. Above the LCST, the shrinkage of microgels may cause a rapid drug release in a short time. Consequently, the drug-loaded microgels may release drugs massively in the lesion location through the local heating.

2.6. Cytotoxicity measurement

Cytotoxicity is an important factor when choosing an appropriate drug delivery vector. The cytotoxicity of P(NIPAAm-*co*-HFMA-*co*-MPEGMA) microgels is evaluated by an MTT viability assay against Caco-2 cells. Fig. 8 shows the Caco-2 cells viability treated with different concentrations of N33F34-PEG33 emulsion.

As shown in Fig. 8, with increasing the concentration of N33F34-PEG33 emulsion, the cell viability decreases gradually, but the cell viability is all kept above 90%. The high cell viability indicates that the N33F34-PEG33 microgels have low toxicity. On the one hand, the network of microgel particles absorbs a larger number of water molecules, which stretches the cross-linked macromolecular chains greatly. Consequently, the microgel particles have a certain fluid property, which improves the affinity between body tissues and copolymers. On the other hand, PEG chains in the copolymers also improve the biocompatibility of the microgels. These factors make the P(NIPAAm-*co*-HFMA-*co*-MPEGMA) microgels have low toxicity.

2.7. Drug loading analysis

In order to study the drug loading capacity of the microgels, 5-fluorouracil is chosen as the hydrophobic model drug [40,41]. It is well known that hydrophobic drugs can be physically incorporated and stabilized in the hydrophobic core by the hydrophobic interaction [42]. In this case, due to the strong hydrophobic PHFMA segments, 5-fluorouracil can be absorbed and stabilized in

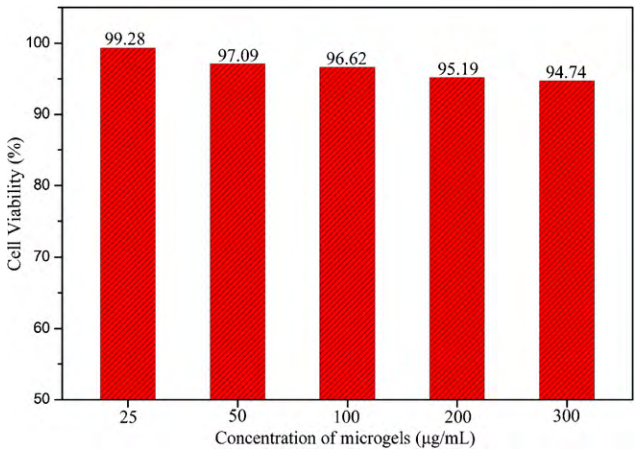

Fig. 8. Caco-2 cells viability treated with different concentrations of N33F34-PEG33 emulsion.

the cores of microgel particles. The dialysis technique against ultrapure water is used to prepare drug-loaded microgels. The mass of drug loaded in the microgels is calculated by measuring the UV absorbance at 265 nm. The experimental results show that 5-fluorouracil is successfully incorporated into microgel particles. For the N33F34-PEG33 microgels, the DLC and EE are about 23.1% and 39.4%, respectively.

2.8. Drug release analysis

To study the effect of temperature on the release of 5-fluorouracil from the N33F34-PEG33 microgels, the prepared drug-loaded microgels are put into two dialysis bags (A and B) and dialyzed against phosphate buffer solutions (PBS) at pH 7.4. A is kept at constant temperature (25 °C), while B is kept at variable temperature (25–49 °C). Fig. 9 shows the cumulative release curves of drug-loaded microgels under different conditions.

For curve (A), there is a slight burst release for initial 10 h, followed by a gradual release up to 24 h, followed by an almost constant release up to 48 h. The final drug release percentage is 27% in the period of 48 h. Because of the hydrophobic interaction between the drugs and fluorine-containing cores of microgel particles, 5-fluorouracil is different to spread to the outside of microgel particles. Besides, the hydrophilic PEG side chains in the shell of particles, which are fully extended below the LCST, stabilize the drugs in the cores. These factors are beneficial to improve the drug loading property of microgels.

For curve (B), the gradual increase of temperature causes the cumulative release of drug-loaded microgels to be higher than that of curve (A) at the same time. Specially, when the temperature reaches the LCST, there is a sharp increase in the cumulative release. However, during the period of 48 h, the final drug release percentage is 66%, which is much higher than that of curve (A). Above the LCST, the obvious shrinkage of microgel particles leads to the much faster drug release than that below the LCST, which is the reason for high release percentage at high temperature. The initial slight burst release in both curve (A) and curve (B) may be attributed to the release of unstable 5-fluorouracil in the shells of microgels.

These results show that the thermo-sensitive P(NIPAAm-*co*-HFMA-*co*-MPEGMA) microgels have potential applications as a controlled drug release carrier, and the loaded drugs may be released massively in the lesion location through the local heating.

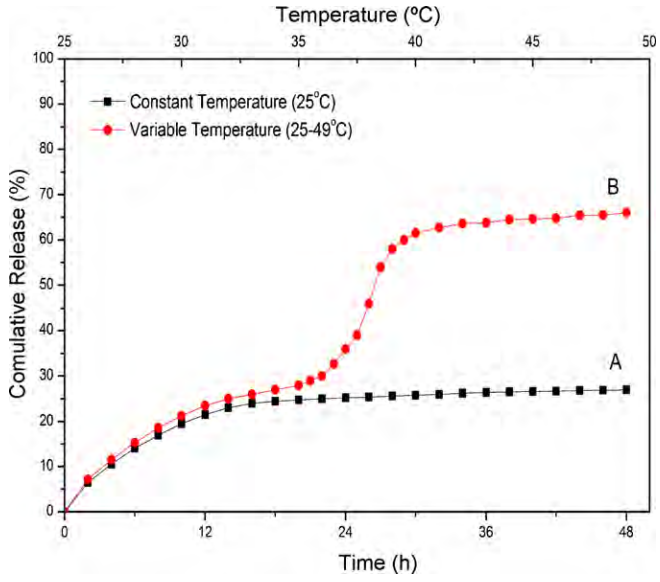

Fig. 9. The cumulative release curves of drug-loaded microgels under different conditions. (A) The sample was kept at constant temperature (25 °C); (B) The sample was kept at variable temperature (25–49 °C).

3. Conclusion

In this work, we have prepared a novel series of fluorine-containing thermo-sensitive core/shell microgel particles P(NIPAAm-*co*-HFMA-*co*-MPEGMA). The structure and composition of the copolymer microgels are characterized by FTIR, ^{1}H NMR and ^{19}F NMR. The thermo-responsive behavior of the microgels is studied by UV–vis spectroscopy, fluorescence spectroscopy, dynamic light scattering, and transmission electron microscopy. The results show that the change of temperature has a significant impact on the morphology and size of microgel particles. MTT viability assay indicates that the copolymer microgels have low toxicity. The drug loading and *in vitro* drug release analysis show that the prepared microgels have a desired thermo-responsive drug release behavior. Our study suggests that the prepared P(NIPAAm-*co*-HFMA-*co*-MPEGMA) microgels have a potential application as an intelligent drug carrier.

4. Experimental

4.1. Materials

N-isopropylacrylamide (NIPAAm) was purchased from Acros Organics (analytical grade) and used as received. 2,2,3,4,4,4-Hexafluorobutyl methacrylate (HFMA) was purchased from Xeogia Fluorine-Silicon Chemical Company (Harbin, China, chemical purity) and distilled under reduced pressure before use. Poly(ethylene glycol) methyl ether methacrylate (MPEGMA) (average molecular weight of 1100 g/mol) was purchased from Sigma-Aldrich and used as received. N,N′-Methylenebisacrylamide (MBA) was purchased from Shanghai Chemical Reagents Co. (Shanghai, China, analytical grade) and used as received. Potassium persulfate (KPS) was purchased from Shanghai Chemical Reagents Co. (Shanghai, China, chemical purity) and purified by recrystallization in ethanol before use. 5-fluorouracil (5-FU) was purchased from the Aladdin and used as received. Ultrapure water was used in all the preparation and characterization processes.

4.2. Preparation of the fluorinated thermo-sensitive microgels

The P(NIPAAm-*co*-HFMA-*co*-MPEGMA) microgels were prepared via surfactant free emulsion polymerization. In a typical reaction, NIPAAm (0.329 g), HFMA (0.341 g), MPEGMA (0.332 g), and H_2O (25 mL) were added into a 50 mL round bottom flask containing a magnetic stirrer. After pre-emulsification for 30 min, MBA (0.03 g) and KPS (0.04 g) were added into the flask. The flask was then deoxygenated under reduced pressure and backfilled with nitrogen several times. Polymerization was carried out at 73 °C for 24 h. After polymerization, the product was put into a dialysis bag (MWCO = 8000–14,000) and dialyzed against 1000 ml ultrapure water at 25 °C for 3 days. The polymerization conversion and solid content were measured by gravimetric analysis. Here, the abbreviation scheme NXFY-PEGZ was used, where X represented the theoretical NIPAAM wt% in the copolymer, Y represented the theoretical HFMA wt% in the copolymer, and Z represented the theoretical MPEGMA wt% in the copolymer. The detailed polymerization conditions were listed in Table 3.

4.3. Apparatus and measurement

4.3.1. Structural characterization

Solid samples of the latexes were obtained from precipitation in ethanol. The filtered latexes were dissolved in a small amount of

THF. Then the mixture was precipitated in n-hexane. After filtration, the precipitate was purified by re-precipitation repeatedly in n-hexane. The obtained product was dried under vacuum at 30 °C for 48 h.

FTIR spectra of the copolymers were recorded on the Perkin-Elmer Spectrum one Transform Infrared Spectrometer (Perkin-Elmer, USA).

All the ^{1}H NMR and ^{19}F NMR spectra were recorded using a UNITY INVOA-600 MHz spectrometer (Varian, USA) with $CDCl_3$ as the solvent at room temperature.

4.3.2. LCST measurement

The LCST (lower critical solution temperature) values of the microgels were determined by measuring the optical transmittance of the copolymer emulsion. The transmittance at various temperatures was measured at 500 nm using a Perkin-Elmer lambda 17 UV–vis spectrophotometer. Sample cell was thermostated for 5 min in a refrigerated circulator bath at various temperatures from 25 °C to 50 °C prior to measurements. The LCST of the microgels were determined at the temperatures showing 50% of the initial transmittance.

4.3.3. Fluorescence spectroscopy

The effect of temperature on the hydrophobicity of the microgels was studied by the fluorescent probe technique using Nile red as the probe. The samples for spectroscopic analysis were prepared as follows. A Nile red stock solution (1 mg/mL) was prepared in distilled water and stored until used. The Nile red (5 μL) solution was placed in a cuvette. Then the copolymer emulsion (1 mg/mL) was added into the cuvette. The fluorescence spectra were recorded on the RF-540 (Hitachi high-technologies corporation, Tokyo, Japan) spectrofluorimeter in the wavelength range of 400–750 nm. The excitation wavelength was 550 nm. Both the excitation and emission slits were 5 nm. Sample cell was thermostated for 5 min in a refrigerated circulator bath at various temperatures prior to measurements.

4.3.4. Dynamic light scattering

The average hydrodynamic diameter and size distribution of the microgel particles were measured by dynamic light scattering (DLS) (Autosize Loc-Fc-963, Malvern Instrument). Measurements were carried out at an angle of 90° with 679 nm wavelength laser light. Sample cell was thermostated for 5 min prior to measurements.

4.3.5. Transmission electron microscopy

The morphology of the microgels was characterized by TEM (Tecnai G20, FEI Corp., USA). The drops of the emulsion (1 mg/mL) were placed on Formvar-coated copper grid. The samples were dried under vacuum at 25 °C and 45 °C, respectively. The TEM images were obtained at an electron acceleration voltage of 200 kV.

4.3.6. Cytotoxicity measurement

The relative cytotoxicity of the microgels was measured by an MTT viability assay against Caco-2 cells. The cells were seeded in 96-well plates at 1×10^4 cells/well and incubated at 37 °C in a 5% CO_2 atmosphere for 24 h. The culture medium was removed and the copolymer emulsion was added into the plates at different concentrations. After the second 24-h incubation, the medium was removed and 20 μL MTT solutions (5 mg/mL) were added into each well. The cells were incubated for another 4 h. Then the supernatant was removed and 150 μL DMSO was added into each well. After 30 min incubation, the whole process of cell cultivation was completed.

The absorbance of this solution was measured at 570 nm using a Microplate reader. The relative cell viability was calculated by the following equation: relative cell viability (%) = (OD_{sample}/$OD_{control}$) × 100, where $OD_{control}$ was obtained in the absence of microgel emulsion and OD_{sample} was obtained in the presence of micogel emulsion.

4.3.7. Drug loading analysis

In order to study the drug loading capacity of the microgels, 5-fluorouracil was chosen as the hydrophobic drug model. 10 mL 5-fluorouracil aqueous solution (2 mg/mL) was added into 10 mL microgel emulsion (2 mg/mL) to achieve a final concentration of 1 mg/mL. After 20 min vortex, the mixture was filtered through 450 nm pore size membrane. Then the mixture was put into a dialysis bag (MWCO = 8000–14,000) and dialyzed against 1000 mL ultrapure water at 25 °C for 3 days to remove the drugs unloaded in the microgel particles.

To determine the drug loading content (DLC) and entrapment efficiency (EE), the absorbance of the drug-loaded microgel emulsion was measured by UV–vis spectrophotometer at 265 nm. The mass of drug loaded in the microgels was calculated by the standard calibration curve experimentally obtained with 5-FU/H_2O solutions. Then the DLC and EE were calculated based on the following formulas:

$$\mathrm{DLC(wt\%)} = \frac{\text{mass of drug loaded in microgels}}{\text{mass of drug} - \text{loaded microgels}} \times 100\%$$

$$\mathrm{EE(wt\%)} = \frac{\text{mass of drug loaded in microgels}}{\text{the initial mass of drug before dialysis}} \times 100\%$$

4.3.8. Drug release analysis

To study *in vitro* drug release, the prepared drug-loaded microgels were put into two dialysis bags (A and B) (MWCO = 8000–14,000) and dialyzed against 1000 mL phosphate buffer solutions (PBS) at pH 7.4. A was kept at constant temperature (25 °C), while B was kept at variable temperature (25–49 °C). Periodically, aliquots of 5 ml of buffered solution outside the dialysis bag were removed for UV–vis analysis and replaced with the same volume fresh PBS in order to hold the volume of solutions constant. The amount of drug released from microgels at different temperatures was measured by UV absorbance at 265 nm.

Acknowledgment

The work was jointly supported by the Key Projects in the National Science & Technology Pillar Program during the Eleventh Five-year Plan Period (No. 2008BAC32B03).

References

[1] H. Nur, V.T. Pinkrah, J.C. Mitchell, L.S. Benee, M.J. Snowden, Adv. Colloid Interface Sci. 158 (2010) 15–20.
[2] L.N. Gu, Z. Shen, C. Feng, Y.G. Li, G.L. Lu, X.Y. Huang, G.W. Wang, J.L. Huang, J. Mater. Chem. 18 (2008) 4332–4340.
[3] B.H. Tan, K.C. Tam, Y.C. Lam, C.B. Tan, Polymer 46 (2005) 10066–10076.
[4] L.N. Gu, C. Feng, D. Yang, Y.G. Li, J.H. Hu, G.L. Lu, X.Y. Huang, J. Polym. Sci. Polym. Chem. 47 (2009) 3142–3153.
[5] V. Lapeyre, C. Ancla, B. Catargi, V. Ravaine, J. Colloid Interface Sci. 327 (2008) 316–323.
[6] I. Widnersson, B.M. Teo, M. Ashokkumar, F. Grieser, Colloids Surf. A 377 (2011) 342–348.
[7] I. Eka, B. Elmas, M. Tuncel, A. Tuncel, Colloids Surf. A 279 (2006) 247–253.
[8] Y. Matsumura, K. Iwai, J. Colloid Interface Sci. 296 (2006) 102–109.
[9] S.G. Chai, J.Z. Zhang, T.T. Yang, J.J. Yuan, S.Y. Cheng, Colloids Surf. A 356 (2010) 32–39.
[10] Y. Zhang, W. Zhu, B.B. Wang, J.D. Ding, J. Controlled Release 105 (2005) 260–268.
[11] J.K. Oh, R. Drumright, D.J. Siegwart, K. Matyjaszewski, Prog. Polym. Sci. 33 (2008) 447–448.

[12] A. Khan, J. Colloid Interface Sci. 313 (2007) 697–704.
[13] W.J. Liu, Y.M. Huang, H.L. Liu, Y. Hu, J. Colloid Interface Sci. 313 (2007) 117–121.
[14] L. Tong, Z. Shen, D. Yang, S. Chen, Y.J. Li, J.H. Hu, G.L. Lu, X.Y. Huang, Polymer 50 (2009) 2341–2348.
[15] S.D. Xiong, L. Li, S.L. Wu, Z.S. Xu, P.K. Chu, J. Polym. Sci. Polym. Chem. 47 (2009) 4895–4907.
[16] H. Liu, Y.J. Li, S. Zhang, D. Yang, J.H. Hu, X.Y. Huang, J. Polym. Sci. Polym. Chem. 49 (2011) 11–22.
[17] M. Liu, Z.S. Fu, Q. Wang, J.T. Xu, Z.Q. Fan, Eur. Polym. J. 44 (2008) 3239–3245.
[18] H.K. Ju, S.Y. Kim, Y.M. Lee, Polymer 42 (2001) 6851–6857.
[19] C. Feng, Y.J. Li, D. Yang, J.H. Hu, X.H. Zhang, X.Y. Huang, Chem. Soc. Rev. 40 (2011) 1282–1295.
[20] J.D. Thomas, G. Fussell, S. Sarkar, A.M. Lowman, M. Marcolongo, Acta Biomater. 6 (2010) 1319–1328.
[21] Y.J. Li, S. Zhang, L. Tong, Q.N. Li, W.X. Li, G.L. Lu, H. Liu, X.Y. Huang, J. Fluorine Chem. 130 (2009) 354–360.
[22] S.D. Xiong, X.L. Guo, L. Li, S.L. Wu, P.K. Chu, Z.S. Xu, J. Fluorine Chem. 131 (2010) 417–425.
[23] L. Tong, Z. Shen, S. Zhang, Y.J. Li, G.L. Lu, X.Y. Huang, Polymer 49 (2008) 4534–4540.
[24] Y.J. Li, S. Chen, S. Zhang, Q.N. Li, G.L. Lu, W.X. Li, H. Liu, X.Y. Huang, Polymer 50 (2009) 5192–5199.
[25] M.G. Dhara, S. Banerjee, Prog. Polym. Sci. 35 (2010) 1022–1077.
[26] H. Liu, S. Zhang, Y.J. Li, D. Yang, J.H. Hu, X.Y. Huang, Polymer 51 (2010) 5198–5206.
[27] D. Yang, L. Tong, Y.J. Li, J.H. Hu, S. Zhang, X.Y. Huang, Polymer 51 (2010) 1752–1760.
[28] M.P. Krafft, Adv. Drug Delivery Rev. 47 (2001) 209–228.
[29] T.H. Qu, A.R. Wang, J.F. Yuan, J.H. Shi, Q.Y. Gao, Colloids Surf. B 72 (2009) 94–100.
[30] X.Z. Zhang, C.C. Chu, Polymer 46 (2005) 9664–9673.
[31] C. Feng, Z. Shen, Y.J. Li, L.N. Gu, Y.Q. Zhang, G.L. Lu, X.Y. Huang, J. Polym. Sci. Polym. Chem. 47 (2009) 1811–1824.
[32] A. Khan, A.M.E. Toni, S. Alrokayan, M. Alsalhi, M. Alhoshan, A.S. Aldwayyan, Colloids Surf. A 377 (2011) 356–360.
[33] C. Feng, Y.J. Li, D. Yang, Y.G. Li, J.H. Hu, S.J. Zhai, G.L. Lu, X.Y. Huang, J. Polym. Sci. Polym. Chem. 48 (2010) 15–23.
[34] X.M. Song, Y.Q. Zhang, D. Yang, L. Yuan, J.H. Hu, G.L. Lu, X.Y. Huang, J. Polym. Sci. Polym. Chem. 49 (2011) 3328–3337.
[35] S.J. Zhai, B.D. Wang, C. Feng, Y.J. Li, D. Yang, J.H. Hu, G.L. Lu, X.Y. Huang, J. Polym. Sci. Polym. Chem. 48 (2010) 647–655.
[36] C.H. Ni, X.X. Zhu, Q.L. Wang, X.Y. Zeng, Chin. Chem. Lett. 18 (2007) 79–80.
[37] S.Q. Liu, Y.W. Tong, Y.Y. Yang, Biomaterials 26 (2005) 5064–5074.
[38] S.D. Xiong, L. Li, J. Jiang, L.P. Tong, S.L. Wu, Z.S. Xu, P.K. Chu, Biomaterials 31 (2010) 2673–2685.
[39] Y.J. Li, S. Zhang, H. Liu, Q.N. Li, W.X. Li, X.Y. Huang, J. Polym. Sci. Polym. Chem. 48 (2010) 5419–5429.
[40] M.B. Sintzel, J. Heller, S.Y. Ng, C. Tabatabay, K.S. Abdellaoui, R. Gurny, J. Controlled Release 55 (1998) 213–218.
[41] O. Garcia, M.D. Blanco, J.A. Martin, J.M. Teijon, Eur. Polym. J. 36 (2000) 111–122.
[42] C.Y. Choi, S.Y. Chae, J.W. Nah, Polymer 47 (2006) 4571–4580.